ELSEVIER

Journal of Photochemistry and Photobiology A: Chemistry 95 (1996) 41–49

Journal of PHOTOCHEMISTRY AND PHOTOBIOLOGY A:CHEMISTRY

The mechanism of photochemical C–O or C–S bond cleavage in aryl(thio)ethers

Gerd Pohlers [a,1], Herbert Dreeskamp [a], Stefan Grimme [b,*]

[a] *Institut für Physikalische und Theoretische Chemie der Technischen Universität Braunschweig, Hans-Sommer Str. 10, D-38106 Braunschweig, Germany*

[b] *Institut für Physikalische und Theoretische Chemie der Universität Bonn, Wegelerstrasse 12, D-53115 Bonn, Germany*

Abstract

By photochemically induced ^{1}H nuclear polarization (^{1}H-CIDNP) spectroscopy, C–O or C–S bond cleavage is confirmed as the primary step in the photolysis of cyanomethyl-1-naphthylether (**1Aa**), cyanomethyl-2-naphthylether (**1Ba**), 2-methylallyl-1-naphthylether (**1Ab**), 1,1-dimethylallyl-2-naphthylthioether (**1Cc**), 1,1-dimethylallyl-2-pyrenylether (**1Dc**) and 1,1-dimethylallyl-3-fluoranthenylether (**1Ec**). The polarization observed in the diamagnetic products formed via the primary aryloxy or naphthylthiyl and cyanomethyl- or methyl-substituted allyl radicals respectively is used to determine the spin multiplicity of the excited precursor states. Both the lowest excited singlet and triplet states are found to be photoreactive. These findings are supported by experiments using radical scavengers, triplet sensitizers or triplet quenchers. The kinetic constants of deactivation of the excited states are derived from the quantum yields, fluorescence decay times and laser flash spectroscopy of the transient triplets and radicals. Except for the rate constant of bond dissociation, these are very similar to those of related photostable methylaryl(thio)ethers. We conclude that bond cleavage is caused by a thermally activated crossing from bonding $S_1(\pi\pi^*)$ and $T_1(\pi\pi^*)$ states into dissociative $\pi\sigma^*$ states in full support of an earlier theoretical study. The experimental conditions determine whether the singlet or triplet channel dominates. The spin densities of the radicals involved and the C–O bond dissociation enthalpies are computed at the semiempirical AM1 level and are correlated with the experimentally observed product distributions and disappearance quantum yields.

Keywords: Photochemically induced ^{1}H nuclear polarization spectroscopy; C–O bond cleavage; C–S bond cleavage; Aryl(thio)ethers

1. Introduction

In previous publications, we reported the photochemistry of (phenoxy)acetophenones [1,2], (4-methoxyphenoxy)-acetone and (*N*-methylanilino)acetone [3] and 1,1-dimethylallyl-1-naphthylether and 1,1-dimethylallyl-2-naphthylether [4] in fluid solution studied by photochemically induced ^{1}H nuclear polarization (^{1}H-CIDNP) spectroscopy and UV absorption and emission spectroscopy. In these reactions, the primary photochemical step is breaking of the C–O or C–N bond [5,6]. Remarkably, however, the spin multiplicity of the precursor state was found to be a singlet or triplet depending on the experimental conditions [3,4]. A molecular orbital (MO) theoretical study of the potential energy surfaces of related model systems interpreted the observed photodissociation as being due to a thermally activated crossing from a bound $n\pi^*$ or $\pi\pi^*$ state into a dissociative $\pi\sigma^*$ state [7].

In this paper, questions following from preceding studies will be investigated. Are analogous phenomena observed by replacing (i) the allyl, benzoylmethyl or acetonyl groups by a cyanomethyl group or (ii) the ether oxygen by sulphur and (iii) by reducing the S_1 and T_1 state energies by selecting larger aryl substituents. Thus we studied the photodissociation of cyanomethyl-1-naphthylether (**1Aa**), cyanomethyl-2-naphthylether (**1Ba**), 2-methylallyl-1-naphthylether (**1Ab**), 1,1-dimethylallyl-2-naphthylthioether (**1Cc**), 1,1-dimethylallyl-2-pyrenylether (**1Dc**) and 1,1-dimethylallyl-3-fluoranthenylether (**1Ec**) by the same techniques as used before. The reactions to be expected from previous work are summarized in Scheme 1. Since all these molecules have emissive S_1 or T_1 states, it is possible to determine the kinetic parameters of the primary photophysical steps from the luminescence spectra and to compare these with the data of related photostable methylaryl(thio)ethers **AM**, **BM**, **CM**, **DM** and **EM**.

To simplify the nomenclature, the following convention for the designation of compounds has been adopted (see Scheme 1 and Table 1): the starting material is identified by

* Corresponding author.

[1] Present address: Department of Chemistry, University of Ottawa, Ottawa, Ont., Canada.

SSDI 1010-6030(95)04239-3

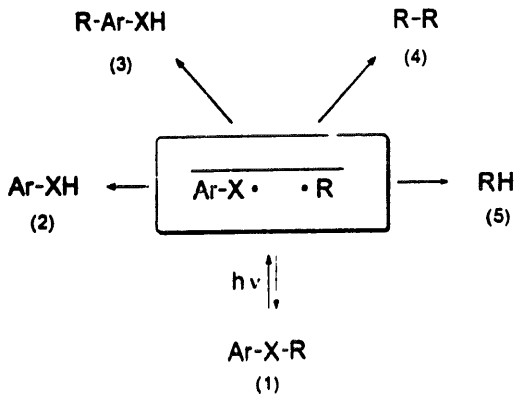

Scheme 1.

the number **1** and the reaction products by consecutive numbers **2–5**; the aromatic fragments are given by capital letters **A, B, C, D** and **E**; the group attached to O or S is denoted by lower case letters **a, b, c** or **M** for the CH_3 group. Thus, for example, cyanomethyl-1-naphthylether is **1Aa**, 1-napithol is **2A**, butanedinitrile is **4aa** and methyl-2-naphthylthioether is **CM**.

2. Experimental details

2.1. Materials

2.1.1. Compound *1Aa*

Cyanomethyl-1-naphthylether was synthesized according to Djerassi and Scholz [12] starting from 1-naphthol (**2A**) and chloroacetonitrile. The crude product was purified by high-vacuum distillation and subsequent fivefold recrystallization from methanol yielding a colourless solid (melting point (m.p.), 74 °C). ^{1}H-NMR (methanol-d_4, 298 K, $\delta(CD_2HOD) = 3.3$ ppm): 5.18 (s, 2H), 7.05 (dd, 1H, $^3J = 7.70$ Hz, $^4J = 0.82$ Hz), 7.39–7.54 (m, 4H), 7.81–7.87 (m, 1H), 8.14–8.21 (m, 1H).

2.1.2. Compound *1Ba*

Cyanomethyl-2-naphthylether was synthesized in analogy with **1Aa**, starting from 2-naphthol (**2B**). The analogous purification procedure yielded a colourless solid (m.p., 76 °C). ^{1}H-NMR: 5.09 (s, 2H), 7.19 (dd, 1H, $^3J = 9.07$ Hz, $^4J = 2.75$ Hz), 7.35–7.50 (m, 3H), 7.78–7.84 (m, 3H).

Table 1
Abbreviations and ESR parameters of the aryloxy (**A, B, D, E**), thioaryl (**C**) and alkyl (**a–c**) radicals relevant for the investigated photoreactions. The experimental g factors and hyperfine coupling constants are from Refs. [8] (**a**), [9] (**b**) and [10] (**c**). The numbers at the atoms denote the percentage spin densities calculated at the AM1-RHF (half-electron method) [11] level of theory

Radical	g-factor	Radical	g-factor	a_H/mT	
				Exp.	AM1-UHF
(A) 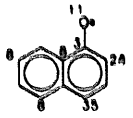	> 2.0029	(a) $\cdot CH_2-C\equiv N$ (79, 21)	2.0029	2.088	−1.90
(B) 	> 2.0029				
(C) 	> 2.0026	(b) 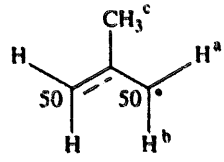	2.0026 [b]	H_a: 1.468 H_b: 1.382 H_c: 0.319	−1.15 −1.48 −0.42
(D) 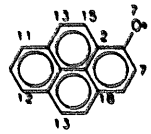	> 2.0026				
(E) 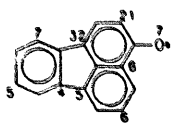	> 2.0026	(c) 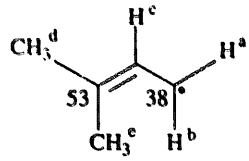	2.0026	H_a: 1.383 H_b: 1.314 H_c: 0.404 H_d: 1.531 H_e: 1.244	−1.38 −1.33 +0.90 +0.194 +1.93

2.1.3. Compound 1Ab

2-Methylallyl-1-naphthylether was prepared according to Burnett and Thomson [13] starting from 3-chloro-2-methyl-1-propene and 1-naphthol (**2A**). The crude product was purified by high-vacuum distillation and subsequent column chromatography yielding a colourless oil (boiling point (b.p.), 100 °C at 2×10^{-6} mbar). ^{1}H-NMR: 1.90 (m, 3H), 4.63 (m, 2H), 5.03 (m, 1H), 5.19 (m, 1H), 6.88 (dd, 1H, ^3J=6.87 Hz, ^4J=1.38 Hz), 7.31–7.49 (m, 4H), 7.75–7.81 (m, 1H), 8.20–8.27 (m, 1H).

2.1.4. Compound 1Cc

1,1-Dimethylallyl-2-naphthylthioether, a compound not yet described in the literature, was synthesized by adding slowly, under reflux, 1-bromo-3-methyl-2-butene dissolved in ethanol to a solution of 2-thionaphthol (**2C**) and potassium hydroxide in ethanol. After 2 h of reaction the product was extracted by ether and purified by column chromatography, yielding **1Cc** as a colourless oil. ^{1}H-NMR: 1.58 (m, 3H), 1.68 (m, 3H), 3.64 (dm, 2H, ^3J=7.70 Hz), 5.32 (tm, 1H, ^3J=7.70 Hz), 7.38–7.49 (m, 3H), 7.73–7.82 (m, 4H).

2.1.5. Compound 1Dc

1,1-Dimethylallyl-1-pyrenylether, a compound not yet described in the literature, was synthesized from 1-bromo-3-methyl-2-butene and 1-pyrenol in analogy with **1Ab**. 1-Pyrenol (**2D**) was synthesized according to Schofield and Schulz [14]. Purification of **1Dc** was performed by column chromatography and recrystallization from methanol yielding a colourless solid (m.p., 53 °C). ^{1}H-NMR: 1.82 (m, 6H), 4.85 (dm, 2H, ^3J=6.71 Hz), 5.65 (tm, 1H, ^3J=6.71 Hz), 7.59 (d, 1H, ^3J=8.55 Hz), 7.82–8.09 (m, 7H), 8.37 (d, 1H, ^3J=9.46 Hz).

2.1.6. Compound 1Ec

1,1-Dimethylallyl-3-fluoranthenylether has not yet been reported in the literature. First, 3-fluoranthenol (**2E**) was prepared according to Shenbor and Cheban [15]. **1Ec** was then synthesized from **2E** and 1-bromo-3-methyl-2-butene in analogy with the procedure described for **1Ab** above. After purification by column chromatography and recrystallization from methanol, **1Ec** was obtained as a light yellow solid (m.p., 82 °C). ^{1}H-NMR: 1.82 (m, 3H), 1.84 (m, 3H), 4.77 (dm, 2H, ^3J=6.60 Hz), 5.63 (tm, 1H, ^3J=6.60 Hz), 6.97 (d, 1H, ^3J=7.70 Hz), 7.25–7.36 (m, 2H), 7.59 (dd, 1H, ^3J=7.29/8.39 Hz), 7.85 (d, 1H, ^3J=7.70 Hz), 7.81–7.92 (m, 2H), 7.98 (dd, 1H, ^3J=7.29 Hz, ^4J=0.69 Hz), 8.06 (dd, 1H, ^3J=8.39 Hz, ^4J=0.69 Hz).

2.1.7. Compound CM

Methyl-2-naphthylthioether was synthesized according to Ref. [16] and purified by sublimation (m.p., 63 °C). ^{1}H-NMR: 2.57 (s, 3H), 7.33–7.48 (m, 3H), 7.61–7.63 (m, 1H), 7.72–7.79 (m, 3H).

2.1.8. Compound DM

Methyl-1-pyrenylether was synthesized in analogy with **1Ab** from methyl iodide and 1-pyrenol (**2D**) (m.p., 90 °C). ^{1}H-NMR: 4.15 (s, 3H), 7.63 (d, 1H, ^3J=8.55 Hz), 7.84–8.14 (m, 7H), 8.38 (d, 1H, ^3J=9.46 Hz).

2.1.9. Compound EM

Methyl-3-fluoranthenylether was synthesized in analogy with **1Ab** from methyl iodide and 3-fluoranthenol (**2E**) (m.p., 158 °C). ^{1}H-NMR: 4.06 (s, 3H), 6.99 (d, 1H, ^3J=7.70 Hz), 7.26-7.37 (m, 2H), 7.61 (dd, 1H, ^3J=7.29/8.39 Hz), 7.82–7.93 (m, 2H), 7.89 (d, 1H, ^3J=7.70 Hz), 7.99 (dd, 1H, ^3J=7.29 Hz, ^4J=0.69 Hz), 8.06 (dd, 1H, ^3J=8.39 Hz, ^4J=0.69 Hz).

2.1.10. Other compounds and solvents

AM (methyl-1-naphthylether) and **BM** (methyl-2-naphthylether) were obtained from Aldrich and were purified by distillation and sublimation/crystallization respectively.

The deuterated solvents methanol-d_4 and DMSO-d_6 were obtained from Aldrich and were used as received. Unless otherwise stated all NMR and quantum yield data refer to methanol solution at 298 K. Comparison with the NMR spectra of authentic substances was used to identify products by their NMR spectra. The phenolic reference compounds were prepared photochemically and extracted as described previously [4].

2.2. Apparatus

UV absorption spectra were recorded on a Shimadzu UV-240 spectrometer. Fluorescence and phosphorescence spectra and phosphorescence decay times were obtained on a Perkin-Elmer MPF-44 spectrometer. Fluorescence decay times were determined by the time-correlated, single-photon technique with iterative deconvolution as described in Ref. [17]. Fluorescence decay times were determined on samples with an optical density at the excitation wavelength of less than 0.1 purged with nitrogen and sealed. The spectra of the transients were detected by a laser flash apparatus described in Ref. [18] using sealed samples for the stable compounds **AM–EM** and a flow-through system for photolabile compounds. Methanol was used in all these experiments.

The ^{1}H-CIDNP techniques are the same as reported in detail previously [4]. A modified 250 MHz FT-NMR spectrometer was used, permitting the in situ irradiation of samples by pulses from a 308 nm excimer laser or a two-stage dye laser [19–21]. Two techniques were used to record ^{1}H-CIDNP spectra: (1) steady state spectra by continuous irradiation of the sample using a long train of laser pulses (see Fig. 1(d)); (2) pre-saturation spectra where a short sequence of laser pulses is preceded by broad-band saturation of all ^{1}H-NMR resonances (see Fig. 1(a)). Samples in precision 5 mm NMR tubes were purged by N_2 and sealed. Disappearance quantum yields were measured as reported in Ref. [3] relative to butyrophenone with an estimated precision of

± 10%. More detailed information on the synthesis, apparatus and assignment of resonances is given in Ref. [22].

3. Results

3.1. Reaction quantum yields

The methylarylethers are photostable on 308 nm laser irradiation at 298 K and $c \approx 0.025$ M in methanol-d_4 inside the field of the 250 MHz NMR spectrometer. Methyl-2-naphthylthioether (**CM**), however, shows a very small disappearance quantum yield of $\phi_R < 0.01$ which will be neglected in the following (this reaction revealed itself by a negative polarized ethane signal in a CIDNP experiment). Under the same experimental conditions, the disappearance quantum yields of allyl- and cyanomethyl(thio)ethers were determined (Table 2). At the relatively high concentrations necessary for the CIDNP experiments, cyanomethyl-2-naphthylether (**1Ba**) slowly forms a white precipitate, assumed to be the 1,4-dimer in analogy with examples in the literature [23]. Thus the ϕ_R value given will represent an upper limit for the reaction quantum yield of bond breaking in this case. For **1Aa**, an increase in ϕ_R with temperature from 0.65 at 273 K to 0.89 at 330 K is observed.

3.2. Photophysics

3.2.1. Absorption, fluorescence and phosphorescence spectra

All photoreactive aryl(thio)ethers exhibit UV absorption, fluorescence and phosphorescence spectra closely resembling those of their related photostable methylaryl(thio)ether counterparts. Fig. 1 shows the spectra of **1Aa** and **AM** as prototype examples.

Table 2 summarizes the energy of the S_1 state, fluorescence quantum yields ϕ_f and fluorescence decay times τ_f in methanol at 298 K and the energy of the T_1 state and phosphorescence decay times τ_p in an EtOH–MeOH (4:1) glass at 77 K. The ϕ_f and τ_f data were used to compute the radiative rate constants of fluorescence k_f at 298 K. The temperature dependence of τ_f is discussed in Section 5.

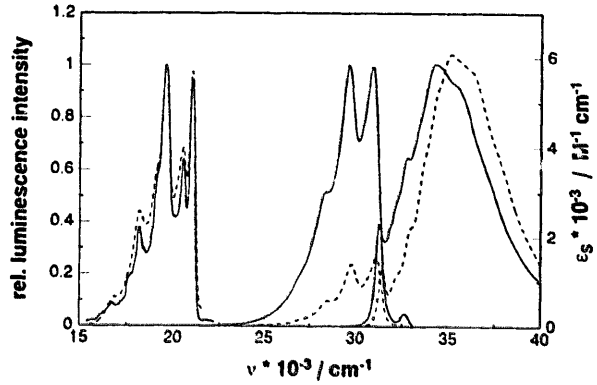

Fig. 1. Absorption, fluorescence (methanol, 298 K) and phosphorescence (methanol–ethanol (4 : 1), 77 K) spectra of compounds **1Aa** (broken line) and **AM** (full line). The fluorescence intensities are on the same scale for **1Aa** and **AM**.

These data clearly prove the $\pi\pi^*$ character of the S_1 and T_1 states as locally excited states of the aryl fragments in all cases.

3.2.2. Laser flash spectroscopy of the transients

For all the aryl compounds investigated, T–T absorption spectra were detected by laser flash spectroscopy. In systems with a sizeable quantum yield ($\phi_R > 0.1$), i.e. **1Aa**, **1Ab** and **1Cc**, an absorption spectrum of another transient with a slower decay time could be observed superimposed on the T–T absorption spectrum. As an example, the time-resolved spectra of **1Aa** are given in Fig. 2.

Comparison with the spectrum of the 1-naphthoxy radical from Ref. [24] and the transient spectrum measured for **AM** identifies the transients as the 1-naphthoxy radical and the T_1

Table 2
Photophysical parameters of the investigated photoreactive compounds and their photostable methylaryl(thio)ether counterparts. $E(S_1)$, τ_f, k_f and ϕ_R are for solutions in methanol at 298 K; $E(T_1)$ and τ_p are for a glass at 77 K

Compound	$E(S_1)$ (kJ mol^{-1})	ϕ_f	τ_f (ns)	k_f (10^7 s^{-1})	$E(T_1)$ (kJ mol^{-1})	τ_p (s)	ϕ_{isc}	$\phi_f + \phi_{isc}$	ϕ_R
1Aa	376	0.11	7.1	1.5	251	1.4	0.15	0.26	0.76
1Ab	375	0.36	13.9	2.6	251	1.6	0.46	0.82	0.18
AM	375	0.42	17.0	2.5	251	1.8	0.54	0.94	0.00
1Ba	370	0.54	18.0	3.0	258	2.2	0.40	0.96	0.10
1Bb	366	0.36	11.5	3.1	260	2.2	0.54	0.90	0.07
BM	366	0.39	12.5	3.1	260	2.2	0.58	0.97	0.00
1Cc	354	0.01	1.1	1.2	246	0.2	–	–	0.65
CM	354	0.03	2.1	1.4	246	0.2	0.80	0.83	<0.01
1Dc	313	0.84	21.6	3.9	195	0.4	0.08	0.92	<0.02
DM	314	0.87	22.8	3.8	195	0.5	0.09	0.96	0.00
1Ec	287	0.35	14.2	2.5	214	0.5	0.56	0.91	0.05
EM	288	0.37	15.2	2.4	215	0.5	0.58	0.95	0.00

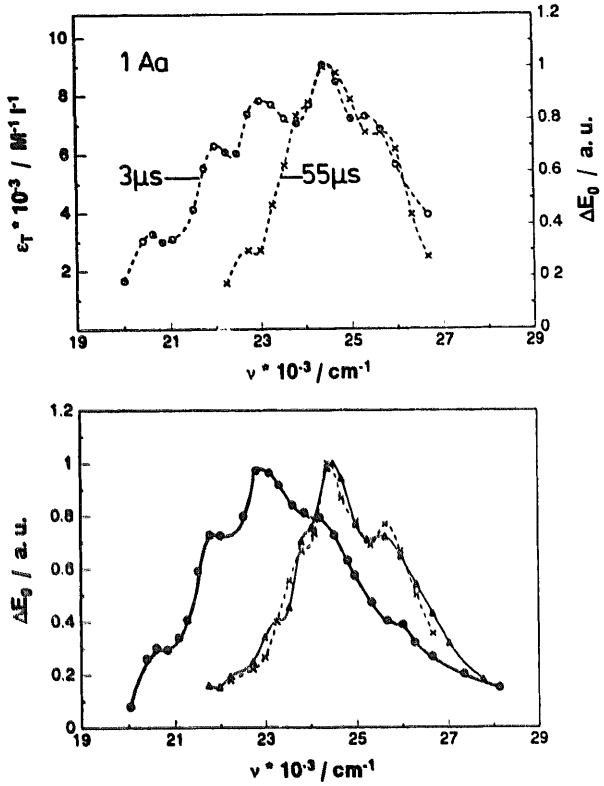

Fig. 2. (a) Transient absorption spectra of **1Aa** observed 3 μs and 55 μs after 308 nm laser pulses. (b) Transient absorption of **AM** (●) and a solution of **1Aa** saturated with O_2 (×) and the absorption spectrum of the 1-naphthoxy radical in acetonitrile from Ref. [24] (▲).

state of **1Aa**. Similarly, the absorption of the 1-naphthoxy radical was found in the laser flash spectrum of **1Ab**, but with a much lower intensity. The transient spectrum of **1Cc** could also be decomposed into a fast component (T–T absorption) and a very intense slow component which we assigned to the 2-naphthylthiyl radical owing to its close resemblance to the 2-naphthoxy radical [25].

The triplet lifetimes τ_T of the photostable reference compounds **AM–EM**, as determined in carefully deoxygenated fluid methanol solution, are found to range from 80 to 160 μs (naphthalene derivatives) and 380 to 460 μs (**EM** and **DM**). In compounds with low ϕ_R values, a decrease in τ_T by a factor of 2–5 relative to the values of the reference compounds is observed. A much stronger effect on τ_T is seen for **1Aa** and **1Cc** (**1Aa** 10 μs, **AM** 150 μs; **1Cc** 5 μs, **CM** 80 μs) which is attributed to bond cleavage from the triplet state in these photolabile molecules. This is consistent with the CIDNP results which suggest a significant contribution of the triplet state reaction to the total disappearance quantum yield in these two compounds.

To determine the quantum yield of $S_1 \rightarrow T_1$ intersystem crossing ϕ_{isc}, the extinction coefficients ϵ_T at the maximum of the T–T absorption were obtained by the energy transfer method [26]. As triplet energy donor, thioxanthone was used for **1Aa**, **1Ab**, **1Ba** and **CM**, biacetyl for **DM** and **1Cc** and chrysene for **EM** and **1Ec**; perylene was used as triplet energy acceptor in the case of **AM** and **BM**. Since no ϵ_T values for the donor or acceptor molecules in methanol are reported in the literature, those given for ethanol [26] or cyclohexane [27] were used. Intersystem crossing quantum yields were determined relative to the standard chrysene in cyclohexane ($\phi_{isc} = 0.85$; $\epsilon(\lambda_{max}) = 21\,600$ (565 nm) [27]) except for **1Dc** and **DM** where anthracene in toluene was used ($\phi_{isc} = 0.72$; $\epsilon(\lambda_{max}) = 42\,000$ (428.5 nm) [26]).

3.3. CIDNP experiments

3.3.1. Cyanomethylnaphthylethers

3.3.1.1. Cyanomethyl-1-naphthylether (1Aa)

As inferred from the product analysis by NMR spectroscopy and from the CIDNP spectra (see Fig. 3), the primary step is cleavage of the C–O bond to yield cyanomethyl (**a**) and 1-naphthoxy (**A**) radicals. Recombination of these radicals produces the two isomeric cyanomethylnaphthols *o*-**3Aa** and *p*-**3Aa** presumably via the short-lived tautomeric cyanomethylnaphthol ions *o*-**3Aa'** and *p*-**3Aa'**. An analogous reaction pathway in the case of the recombination of phenoxy and benzoylmethyl radicals has been found by time-resolved NMR spectroscopy [2]. Two cyanomethyl radicals lead to butanedinitrile (**4aa**) as an escape product. Finally, 1-naphthol (**2A**) and acetonitrile-*d* (**5a**) are formed from 1

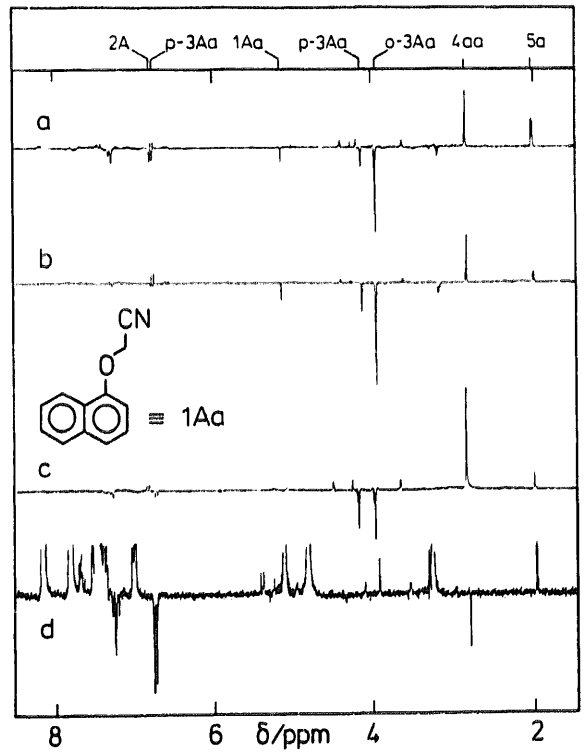

Fig. 3. ^{1}H-CIDNP spectra of 1-cyanomethyl-1-naphthylether (**1Aa**), $c = 0.025$ M: (a) presaturated CIDNP spectrum, methanol-d_4, 298 K; (b) presaturated CIDNP spectrum, methanol-d_4, with 1,3-cyclohexadiene (0.15 M); (c) presaturated CIDNP spectrum, DMSO-d_6, 398 K; (d) steady state CIDNP spectrum, methanol-d_4, 298 K, with $c = 3.3 \times 10^{-3}$ M thioxanthone and excitation at $\lambda = 405$ nm.

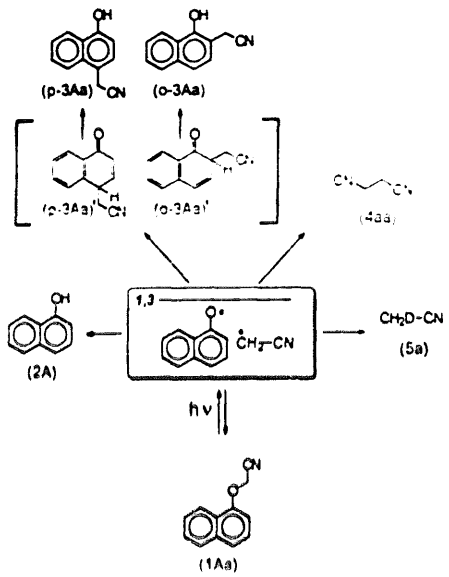

Scheme 2.

naphthoxy and cyanomethyl radicals presumably by hydrogen or deuterium abstraction.

Scheme 2 summarizes these observations. Support of a radical mechanism is given by the ^{1}H-NMR polarizations observed for most of the products (see Fig. 3(a)). Contrary to other CIDNP detected radical reactions, we observe only a small polarization of the starting material which is assigned to a low geminal recombination quantum yield.

To determine the spin multiplicity of the excited precursor state, Kaptein's rule [28] was applied as in the preceding publications [1–4]. The electron spin resonance (ESR) parameters a_H and Δg are given in Table 1. On an electronic structural level, all aromatic radicals show a strong resemblance to the phenoxy radical (see Section 4) which has a large g value of 2.0053 [29]. Thus we assume that the g values of the aryloxy and naphthylthiyl radicals are larger than those of the cyanomethyl or allyl radicals respectively. To determine the parameter ϵ (positive sign for a cage product, negative sign for an escape product), a radical scavenging experiment was performed. Adding 0.025 M tri-*n*-butyltinhydride to a sample greatly reduces the polarization of **4aa** and leaves the polarization of *o*-**3Aa** and *p*-**3Aa** nearly unaffected (spectrum not shown). Thus the naphthols are cage products while butanedinitrile (**4aa**) is confirmed to be an escape product. With this information, Kaptein's rule (see Table 3) leads to a singlet precursor. This result could be confirmed in a separate experiment avoiding the use of Kaptein's rule. We added 1,3-cyclohexadiene as a triplet state quencher. This molecule does not absorb at 308 nm ($E(S_1) = 410$ kJ mol^{-1} [30]) but has a low triplet state energy ($E(T_1) = 230$ kJ mol^{-1} [30]). This is below $E(T_1)$ of **1Aa** (Table 2) and allows efficient energy transfer under the experimental conditions. As shown in Fig. 3(b), the polarization of the cage product **3Aa** has increased, suggesting that in the experiment without a triplet quencher (Fig. 3(a)) the polarization observed is the net polarization of contributions due to the triplet and singlet precursors. Thus we performed an experiment with thioxanthone as triplet sensitizer ($E(S_1) = 310$ kJ mol^{-1}, $E(T_1) = 250$ kJ mol^{-1} [31]) with excitation by 406 nm laser pulses. As shown in Fig. 3(d), the same products are observed with inverted polarization for the cage product **3Aa** and the escape product **4aa** (Table 3). Apparently the same photoreaction of **1Aa** may proceed via the S_1 or T_1 state. Finally, the influence of temperature on the reaction was investigated. Lowering the temperature to 248 K leads to inversion of the polarization sign of the resonances due to the cage product **3Aa** and the escape product **4aa** (see Table 3, spectra not shown), while increasing the temperature to 348 K produces the same sign of polarization (Fig. 3(c)) as observed at room temperature.

3.3.1.2. Cyanomethyl-2-naphthylether (1Ba)

In contrast with **1Aa**, the naphtholic recombination product in the 4-position (i.e. analogous to *p*-**3Aa**) is not formed. The observation of polarized signals of *o*-**3Ba**, **4aa** and **5a** establishes an analogous reaction scheme to **1Aa**. To identify the precursor spin multiplicity, polarization was measured in the presence of tri *n*-butyltinhydride to suppress the escape polarization. The positive sign of the CH_2 group signals in *o*-**3Ba** and negative polarization in **4aa** demonstrate a dominant singlet precursor. Finally, from experiments with a triplet quencher added (1,3-cyclohexadiene, 0.15 M) and at elevated temperatures (DMSO-d_6, 383 K), we conclude that, at low temperatures, the triplet channel contributes to the polarization, whereas at higher temperatures the singlet channel dominates.

3.3.2. Allylarylethers

3.3.2.1. 2-Methylallyl-1-naphthylether (1Ab)

The signals of the products 1-naphthol (**2A**), *o*- and *p*-2-methylallyl-1-naphthol (*o*-**3Ab** and *p*-**3Ab**) and 2,5-dimethylhexadiene (**4bb**) all appear polarized. A reaction scheme analogous to Scheme 2, with the cyanomethyl group replaced by the 2-methylallyl group, applies. From the polarization

Table 3
Assigned polarizations in the ^{1}H-CIDNP spectra of cyanomethyl-1-naphthylether (**1Aa**). Γ_{298} is the sign of the polarizaiton at 298 K (Fig. 3(a)), Γ_{quen} is the sign of the polarization with 1,3-cyclohexadiene added as quencher (Fig. 3(b)), Γ_{253} is the sign of the polarization at 253 K (Fig. 3(c)) and Γ_{sens} is the sign of the polarization while exciting thioxanthone as triplet sensitizer (Fig. 3(d))

Product	Fragment	δ (ppm)	$\Gamma_{298} = \mu \cdot \epsilon \cdot \Delta g \cdot a$	Γ_{quen}	Γ_{253}	Γ_{sens}
(**2A**)	Ortho H	6.79	⊖	⊖	⊖	⊖
(*o*-**3Aa**)	$-CH_2-$	3.97	⊖ = − + − −	⊖	⊕	⊕
(*p*-**3Aa**)	$-CH_2-$	4.15	⊖ = − + − −	⊖	⊕	⊕
	Ortho H	6.78	⊕ = − + + −	⊕		⊖
(**4aa**)	$-CH_2-CH_2-$	2.84	⊕ = − − − −	⊕	⊕	⊖
(**5a**)	$-CH_2D-$	2.01	⊕	⊕	⊕	⊕

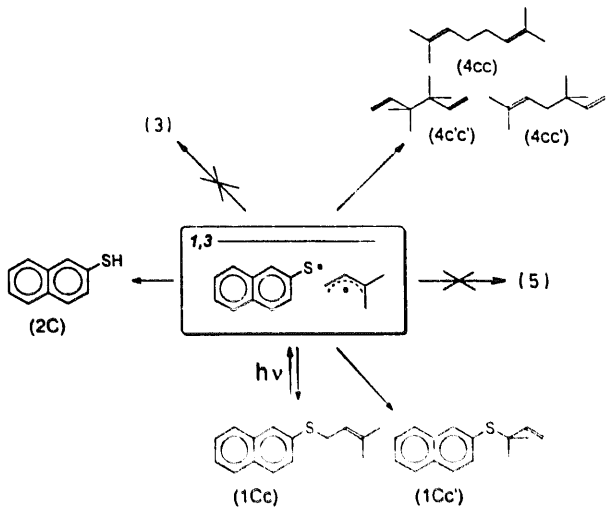

Scheme 3.

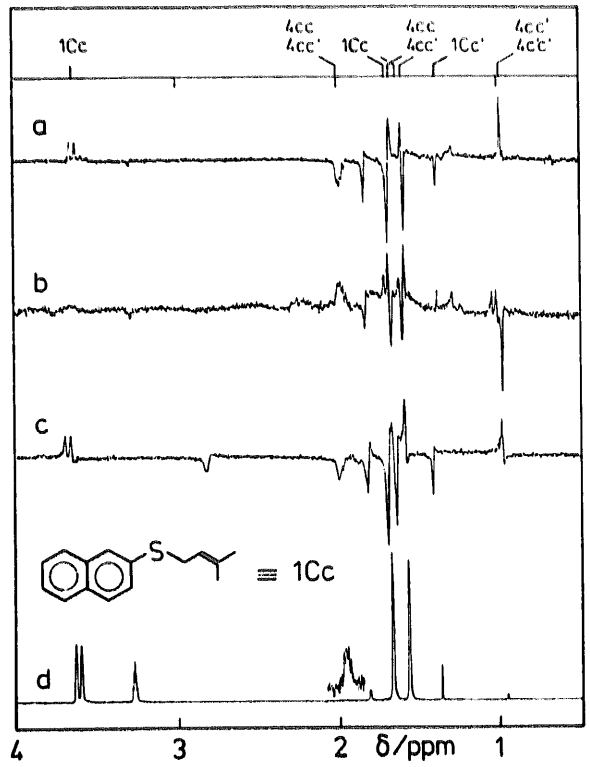

Fig. 4. High field part of the ^{1}H-CIDNP spectra of 1,1-dimethylallyl-2-naphthylthioether (**1Cc**), c = 0.025 M: (a) presaturated CIDNP spectrum, methanol-d_4, 298 K; (b) presaturated CIDNP spectrum, methanol-d_4, with 1,3-cyclohexadiene (0.15 M); (c) presaturated CIDNP spectrum, DMSO-d_6, 423 K; (d) dark spectrum after 5 min irradiation.

sign of the resonances, a triplet precursor is inferred at 298 K. By adding the triplet quencher 1,3-cyclohexadiene to the sample as before, the signals of *o*-**3Ab**, *p*-**3Ab** and **4bb** are inverted (see Table 3). Since, in this experiment, the excited precursor state is predominantly of singlet multiplicity, the polarizations in the previous experiment must be a superposition due to singlet and triplet reaction channels. Moreover, when performing the experiment at 393 K, polarizations are opposite to those at room temperature and equal to those with a triplet quencher, indicating a dominant singlet precursor state at elevated temperatures.

3.3.2.2. 1,1-Dimethylallyl-2-pyrenylether (1Dc)

Although this compound is photolysed with a minute disappearance quantum yield, in the steady state CIDNP spectra polarized signals of the dimerization products of the 1,1-dimethylallyl radicals could be detected. This again proves that homolytic C–O bond dissociation is the primary reaction step. The application of Kaptein's rule leads to a dominant singlet precursor at room temperature. Attempts to confirm this result by either quenching or sensitizing the triplet state failed due to poor signal intensities.

3.3.2.3. 1,1-Dimethylallyl-3-fluoranthenylether (1Ec)

CIDNP signals are observed for 3-fluoranthenol (**2E**) and the isomeric dienes **4cc**, **4cc'** and **4c'c'** (see Scheme 3) confirming C–O bond breaking as the primary reaction step. The application of Kaptein's rule leads to a triplet precursor. When raising the temperature to 423 K with DMSO as solvent, all signals due to the dienes are inverted, showing that at high temperatures the singlet channel dominates the observed polarization.

3.3.3. Allyl-2-naphthylthioether

For 1,1-dimethylallyl-2-naphthylthioether (**1Cc**), polarized signals of the starting material **1Cc**, the rearranged starting material **1Cc'**, 2-thionaphthol (**2C**) and the three isomeric dienes **4cc**, **4cc'** and **4c'c'** (see Fig. 4 and Scheme 3) confirm that S–C bond cleavage is the primary step producing a radical pair. In contrast with the ethers dealt with above, however, no recombination of the radical pair in the 1-, 3- or 4-position of the naphthalene ring is observed. Taking **1Cc** and **1Cc'** to be cage products, Kaptein's rule leads to a predominant triplet precursor as detailed in Table 4. On addition of 1,3-cyclohexadiene to the sample, all polariza-

Table 4
Assigned polarizations in the ^{1}H-CIDNP spectra of 1,1-dimethylallyl-2-naphthylthioether (**1Cc**). Γ_{298} is the sign of the polarization at 298 K (Fig. 4(a)), Γ_{quen} is the sign of the polarization with 1,3-cyclohexadiene added as quencher (Fig. 4(b)) and Γ_{423} is the sign of the polarization at 423 K in DMSO-d_6 (Fig. 4(c))

Product	Fragment	δ (ppm)	$\Gamma_{298} = \mu \cdot \varepsilon \cdot \Delta g \cdot a$	Γ_{quen}	Γ_{423}
(1Cc)	$-CH_3$	1.58	⊖ = + + − +	⊕	⊖
	$-CH_3$	1.68	⊖ = + + − +	⊕	⊖
	$-CH_2-$	3.64	⊕ = + + − −	⊖	⊕
(1Cc')	$C(CH_3)_2$	1.37	⊖ = + + − +	⊕	⊖
(4cc)	$-CH_3$	1.59	⊕ = + − − +	⊖	⊕
	$-CH_3$	1.66	⊕ = + − − +	⊖	⊕
	$-CH_2-CH_2-$	2.01–1.96	⊖ = + − − −	⊕	⊖
(4cc')	$C(CH_3)_2$	0.96	⊕ = + − − +	⊖	⊕
	$-CH_3$	1.59	⊕ = + − − +	⊖	⊕
	$-CH_3$	1.69	⊕ = + − − +	⊖	⊕
	$-CH_2-$	2.0	⊖ = + − − −	⊕	⊖
(4c'c')	CH_3	0.96	⊕ = + − − +	⊖	⊕

tions are inverted (see Fig. 4(b)) indicating the presence of a singlet precursor. When the temperature is raised to 423 K, the triplet channel still dominates the polarization in contrast with the naphthylethers discussed above.

3.4. Spin densities, hyperfine coupling constants and dissociation energies

In an attempt to interpret the observed quantum yields of bond dissociation ϕ_R and product distributions in the secondary radical recombination reactions, we have computed the C–O bond dissociation enthalpies ΔH_R and spin densities of the radicals at the semiempirical restricted Hartree–Fock (RHF) level of theory (all compounds have been completely geometry optimized; spin densities and heat of formation data of the radicals are obtained from an RHF (half-electron method) treatment; all calculations have been performed with the *MOPAC 6.0* program) [11,32]. For the naphthylethers **1Aa** and **1Ba**, ΔH_R values of 192 and 213 kJ mol^{-1} respectively are found, while much lower values of 172 and 175 kJ mol^{-1} respectively are calculated for the larger aromatic systems **1Dc** and **1Ec**. The replacement of the cyanomethyl group with a 2-methylallyl or dimethylallyl group decreases the ΔH_R values by 6–14 kJ mol^{-1} (**1Ab**, 186 kJ mol^{-1}; **1Ac**, 178 kJ mol^{-1}; **1Bb**, 207 kJ mol^{-1}; **1Bc**, 199 kJ mol^{-1}) showing the lower stability of the cyanomethyl radical. This is in agreement with literature data where C–H dissociation energies of 389 kJ mol^{-1} ($NCCH_2$–H) and 362 kJ mol^{-1} (CH_2CHCH_2–H) are reported [33]. Inspection of Table 2 shows that reaction of the excited molecules to give a ground state radical pair by breaking of the C–O bond is highly exothermic, varying from −184 kJ mol^{-1} (S_1, **1Aa**) to −23 kJ mol^{-1} (T_1, **1Dc**).

Additionally, we have computed the hyperfine coupling constants for the allyl radicals at the AM1-UHF level to obtain their signs which are not known experimentally (see Table 1). The absolute values agree very well with the experimental data and the signs agree with those found in a more sophisticated ab initio CI treatment [34].

4. Discussion

The values of τ_f and τ_p given in Table 2 conclusively prove that the S_1 and T_1 states of the photoreactive and photostable compounds are of $\pi\pi^*$ character in all cases. Most significantly, since the lifetimes of the S_1 states inferred from τ_f, and of the T_1 states inferred from the T–T absorption spectra, are relatively long in the photoreactive molecules, we can conclude that these states are non-dissociative. Since, however, bond dissociation is observed via these states, there must be a thermally activated crossing into dissociative states at elevated temperatures. As a consequence, a value of $\phi_f + \phi_{isc} = 1$ is observed within experimental precision only for the photostable compounds, whereas for the photoreactive compounds $\phi_f + \phi_{isc} + \phi_R \approx 1$. Since after photoexcitation the S_1 state is reached first, the CIDNP polarization due to the singlet channel is expected to become dominant (as observed for **1Aa**, **1Ba**, **1Ab** and **1Ec**) if at elevated temperatures the rate constant of dissociation from the S_1 state (^1k_D) increases more strongly than competing desactivation processes as observed. We have estimated ^1k_D and its temperature dependence in the case of **1Ab** and **1Cc** using the same assumptions as in the preceding publication [4]. Essentially these are as follows: since there is a close agreement between the spectra and radiative rate constants k_f of **1Ab** and its photostable counterpart **AM** (and **1Cc** and **CM**) (see Table 2), we assume equal deactivation rate constants of the S_1 states in **1Ab** and **AM** (and **1Cc** and **CM**), with the exception of an additional rate constant of bond cleavage ^1k_D in **1Ab** and **1Cc**. Temperature-dependent fluorescence decay times τ_f in **1Ab**, **AM**, **1Cc** and **CM** were used to determine the rate constant of the dissociation channel from the S_1 state using formulae (4) and (5) of Ref. [4]. The values determined at 298 K are ^1k_R(**1Ab**) = 2×10^7 s^{-1} and ^1k_R(**1Cc**) = 5×10^8 s^{-1} with the Arrhenius parameters ^1A_R(**1Ab**) = 1×10^{11} s^{-1}, ^1E_R(**1Ab**) = 13 ± 2.5 kJ mol^{-1} and ^1A_R(**1Cc**) = 1×10^{11} s^{-1}, ^1E_R(**1Cc**) = 21 ± 3.0 kJ mol^{-1}.

The low fluorescence quantum yield ϕ_f determined for **1Cc** and **CM** is presumed to be due to an internal heavy atom effect. The resulting fast population of the T_1 state can reasonably be expected to lead to a dominant triplet reaction in perfect agreement with the polarization observed in the CIDNP experiments.

The observed reaction quantum yields correlate with the reaction enthalpies of bond dissociation. For example, **1Ba** has a lower quantum yield ($\phi_R = 0.10$, $\Delta H_R = 213$ kJ mol^{-1}) than **1Aa** ($\phi_R = 0.76$, $\Delta H_R = 192$ kJ mol^{-1}). As outlined in detail in Ref. [7], this is expected for a comparison of compounds with similar excitation energies, since an "earlier" crossing (which results in a lower barrier) of the bound $\pi\pi^*$ and dissociative $\pi\sigma^*$ states occurs if the product states are lower in energy. The larger aromatic systems **1Ec** and **1Dc** show lower ΔH_R values (172 kJ mol^{-1} and 175 kJ mol^{-1}), but their singlet excitation energies are also lowered by 60–80 kJ mol^{-1} relative to **1Aa**. Presumably this effect overcompensates the higher radical stability of larger aryloxy radicals so that a very small reaction quantum yield is found.

The product distributions of the secondary radical recombination reactions found in the CIDNP experiments are easily explained by the spin densities of the aryloxy and thionaphthyl radicals (see Table 1). It is generally assumed that the recombination of two radicals is a fast reaction with a negligible reaction barrier if no steric interactions and a high spin density at the corresponding atomic positions are present. The electronic structure of the aromatic radicals can be derived from the phenoxy radical, where the singly occupied molecular orbital (SOMO) is of delocalized π character. In the 1-naphthoxy radical, the spin density is mainly centred at the ortho and para positions relative to the O atom and only a negligible amount is found in the unsubstituted ring and at the O atom (11%). In agreement with this finding, we

observe only two recombination products for **1Aa** and **1Ab** and a small CIDNP signal for the starting material (geminal recombination). For **1Ba**, only one recombination product in the ortho position (37% spin density) is found and no signals of a second ortho or meta recombination product are observed (spin densities are 6% and less than 1%). The situation in the naphthylthiyl radical is significantly different. Here, the spin density is predominantly centred at the S atom (45%), which is demonstrated by a large fraction of the geminal recombination reaction and no observation of compound *o*-**3Cc**. In the larger pyrenyloxy and fluoranthenyloxy radicals, the spin density is spread over the whole π system which may explain, in addition to the low quantum yields, the very small CIDNP intensities found. There are two possible explanations: (i) the polarization is distributed over too many products; (ii) the low spin density at each position prevents recombination so that the polarization is destroyed by relaxation.

5. Conclusions

The experimental results of this and previous work on dimethylallylnaphthylethers [4] prove conclusively that C–O or C–S bond breakage is the primary photochemical step in these systems. Both the singlet and triplet states are photoreactive, with the singlet state reaction gaining in importance at elevated temperatures. These data provide further support to the theoretical study of the homolytic photodissociation of C–O bonds in molecules of the structure R–OPh [7]. In Ref. [7], it was shown that the reaction occurs by a thermally activated crossing from the bonding S_1 or T_1 states with $n\pi^*$ or $\pi\pi^*$ character into a dissociative $\pi\sigma^*$ state. We conclude from our observations that essentially the same interpretation is applicable when (i) the allyl group is replaced by a cyanomethyl group, (ii) the ether oxygen is replaced by a sulphur atom and (iii) due to an extended aromatic π system the excitation energy is quite low. The state correlation diagram and potential energy curves computed in Ref. [7] for allylphenylether and given in fig. 8 of that publication may thus allow a qualitative interpretation to be made of the observations presented in this work.

The subsequent reactions of the primary radical pair to yield the starting material or the different recombination isomers appear to be governed by the spin distribution in the aryl radicals.

Finally, we wish to point out that photoreactions which proceed via the singlet state (as established here) may be used with some advantage in applications: (i) singlet states do not have to sacrifice a large part of the quantum energy in intersystem crossing in contrast with triplet states; (ii) the short lifetime makes the excited singlet states much more immune to inadvertent quenchers compared with triplet states. Thus our compound 1,1-dimethylallyl-3-fluoranthenylether (**1Ec**) is photolysed with violet light to give a radical pair, albeit with a low quantum yield.

Acknowledgements

Support of this work by the Deutsche Forschungsgemeinschaft and the Fonds der Chemischen Industrie is gratefully acknowledged. We thank F. Schael for help with the laser flash experiments.

References

[1] W.U. Palm and H. Dreeskamp, *J. Photochem. Photobiol. A: Chem., 52* (1990) 439.
[2] W.U. Palm, H. Dreeskamp, H. Bouas-Laurent and A. Castellan, *Ber. Bunsenges. Phys. Chem., 96* (1992) 50.
[3] S. Grimme and H. Dreeskamp, *J. Photochem. Photobiol. A: Chem., 65* (1992) 371.
[4] G. Pohlers, S. Grimme and H. Dreeskamp, *J. Photochem. Photobiol. A: Chem., 79* (1994) 153.
[5] H. Shizuka, *Bull. Chem. Soc. Jpn., 42* (1969) 52.
[6] F.A. Carrol and G.S. Hammond, *Israel J. Chem., 10* (1972) 613.
[7] S. Grimme, *Chem. Phys., 163* (1992) 313.
[8] P.J. Krusic, P. Meakin and B.E. Smart, *J. Am. Chem. Soc., 96* (1974) 6211.
[9] P.J. Krusic and J.K. Kochi, *J. Am. Chem. Soc., 90* (1968) 7157.
[10] R. Livingston and H. Zeldes, *J. Magn. Res., 1* (1969) 169.
[11] M.J.S. Dewar, E.G. Zoebisch, E.F. Healy and J.J.P. Stewart, *J. Am. Chem. Soc., 107* (1985) 3902.
[12] C. Djerassi and C.R. Scholz, *J. Am. Chem. Soc., 69* (1947) 1688.
[13] A.R. Burnett and R.H. Thomson, *J. Chem. Soc. (C)*, (1968) 854.
[14] E. Schofield and R.C. Schulz, *Makromol. Chem., Rapid Commun., 2* (1981) 677.
[15] M.I. Shenbor and G.A. Cheban, *Zh. Org. Khim., 5* (1969) 143.
[16] Autorenkollektiv, *Organikum*, Vol. 16, Auflage, VEB Deutscher Verlag der Wissenschaften, Berlin, 1986.
[17] H. Dreeskamp, T. Salthammer and A. Läufer, *J. Lumin., 44* (1989) 161.
[18] T. Kircher, *Ph.D. Thesis*, Technische Universität Braunschweig, 1993.
[19] M. Läufer and H. Dreeskamp, *J. Magn. Res., 60* (1984) 357.
[20] M. Goez, *Chem. Phys., 147* (1990) 143.
[21] M. Goez, *Chem. Phys. Lett., 188* (1992) 451.
[22] G. Pohlers, *Ph.D. Thesis*, Technische Universität Braunschweig, 1995.
[23] B.K. Selinger and M. Sterns, *Chem. Commun.*, (1969) 978.
[24] R. Nakagaki, M. Hiramatsu, T. Watanabe, Y. Tanimoto and S. Nagakura, *J. Phys. Chem., 89* (1985) 3222.
[25] M. Yamaji, T. Sekiguchi, M. Hoshino and H. Shizuka, *J. Phys. Chem., 96* (1992) 9353.
[26] A. Maciejewski and J. Wojtczak, *J. Chem. Soc., Faraday Trans. 2, 80* (1984) 411.
[27] R. Bensasson and E.J. Land, *Trans. Faraday Soc., 67* (1967) 1904.
[28] R. Kaptein, *Adv. Free Rad. Chem., 5* (1975) 319.
[29] F. Graf, K. Loth and H.-H. Günthard, *Helv. Chim. Acta, 60* (1977) 710.
[30] N.J. Turro, *Modern Molecular Photochemistry*, Benjamin Cummings, Menlo Park, 1978.
[31] I. Carmichael and G.L. Hug, *J. Phys. Chem. Ref. Data, 15* (1986) 1.
[32] J.J.P. Stewart, *QCPE Bull., 5* (1985) 133.
[33] S.L. Murov, J. Carmichal and G.L. Hug, *Handbook of Photochemistry*, Marcel Dekker, New York, 2nd edn., 1993.
[34] D.M. Chipman, in S.R. Langhoff (ed.), *Quantum Mechanical Electronic Structure Calculations with Chemical Accuracy*, Kluwer Academic Publications, Dordrecht, 1995, p. 109.